

## MANUFACTURING THROUGH MILLENNIA: A STRUCTURAL INVESTIGATION OF ARCHIMEDES SCREWS

Scott C. Simmons<sup>1</sup>, William David Lubitz<sup>2\*</sup>

<sup>1</sup>Greenbug Energy Inc., Delhi, Canada

<sup>2</sup>School of Engineering, University of Guelph, Guelph, Canada

\*wlubitz@uoguelph.ca

**Abstract**—Archimedes screws are most commonly used in robust pumping and dewatering schemes, and for hydropower generation. Though they have been in use for almost three millennia, there is no investigation of their structural mechanics present in the published literature. This study presents novel techniques that were used to experimentally quantify deflection on an Archimedes screw under varying load conditions. A first-of-kind finite element analysis (FEA) model of an Archimedes screw was developed. The experimental results were used to evaluate the accuracy of the FEA model, and the model was then used to explore the impacts that varying the number of screw blades on the structural response in an Archimedes screw.

**Keywords**—*structural mechanics; experiments; finite element analysis; numerical simulation;*

### I. INTRODUCTION

The Archimedes screw pump (ASP) is an ancient pumping technology; it has been described as the oldest positive displacement pump [1]. Though ASP technology has been implemented for millennia, at the time of publication there was no published literature describing the structural mechanics of ASP design. Only a few empirical and heuristic models have been presented to consider deflection and thermal expansion [2], though no supporting data or documentation was presented. This study sought to address this knowledge gap by presenting preliminary experimentation and early structural modelling efforts. The goal was to investigate the response of Archimedes screws under varying static loading conditions in an effort to better understand deflection within an Archimedes screw.

The Archimedes screw's namesake is the ancient Greek mathematician Archimedes of Syracuse. There is no evidence that Archimedes claimed to invent the device, though it has often been attributed to him by other historical authors (Athenaeus, Diodorus, etc.) when describing its application for irrigating the Nile Delta in the 3rd century BCE [3], draining mines in the Hispania provinces of the Roman Republic and Empire [4], as the first recorded bilge-pump on a 3rd century BCE Syracusan

naval flagship [5], and when describing design iterations and improvements [6, 7]. Though its true origins appear lost to history, evidence suggests the technology was likely developed in Lower Egypt, or in the Neo-Assyrian Empire (c. 7th century BCE) [8]. Archimedes likely learned of the device when studying at the University of Alexandria in the 3rd century BCE.

With such a storied history, the Archimedes screw has seen many applications and design iterations. It has been used as a pump for land drainage [9], wastewater [2], grains and granular solids [10], and to pump hatchery-raised fish while restocking water bodies [11]. It has also been employed for ship propulsion [12], to propel amphibious [13] and marginal terrain vehicles [14], as a pump for injection moulding [15], in heart valve replacements [16], and for hydropower generation [17].

Design of ASPs has changed since their first documented use. Assyrian king Sennacherib (704-681 BCE) wrote an inscription in Akkadian on a clay prism that described his palace, palace gardens, water control methods, and bronze castings used for water control. Based on the context of the text, Dalley [8] interpreted the inscription as describing helical water screws cast of bronze and used to raise water at a palace in Ninevah. Though no dimensions were given, Dalley notes that if the cast screws were similar dimensions to later Egyptian, Greek, and Roman screw pumps, it is estimated that they would have weighed between 2 to 3 tons [8].

The first indisputably documented screw pumps were likely constructed from wood, ceramic, or copper piping [18]. These screw pumps were effectively a helical coil of piping (see Figure 1). No evidence was found regarding the drive mechanism for earlier screw pumps, though they are often depicted in anachronistic illustrations with a hand-crank. Regardless of the drive mechanism, it was documented that the earliest screw pumps were operated by one person [5].

Vitruvius described a later screw pump design in his Ten Books on Architecture (De Architectura) [7]. In the treatise, he outlined the early construction of what is now called an enclosed Archimedes screw pump (see Figure 2). The described water screw was manufactured with a long, straight beam (like a ships

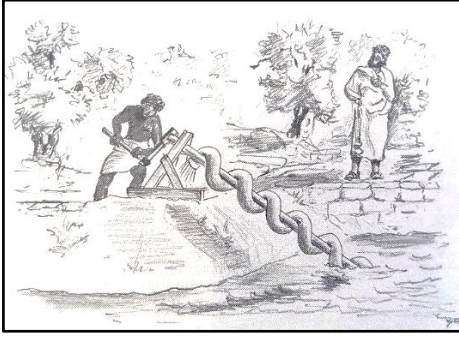


Figure 1. Traditional representation of the Archimedes screw pump, from [12].

mast), willow withes (or similarly flexible, straight wood), boards, and liquid pitch (resin) [7]. The willow withes were soaked in pitch and wound helically around the central beam. Afterwards, pitch-soaked willow withes were added on top of the windings, serving to increase the height of the blades in the radial direction. This was continued until a desired total diameter was reached. The newly fabricated blades were then covered with pitch-soaked boards, fastened at points along their length with iron strapping (like a wooden barrel), and placed between two crossbeams by rudimentary journal bearings at a desired inclination [7].

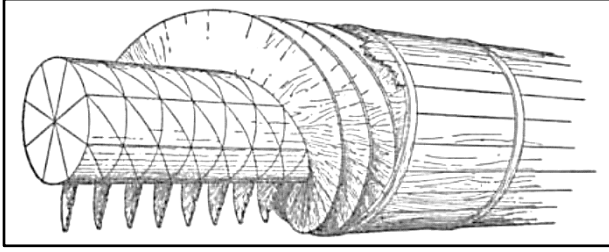


Figure 2. "Construction of the water screw" from Vitruvius [6].

Modern screw pumps may still be manufactured with an enclosed trough similar to Vitruvius' design [2], though it is more common for pumping stations to implement a fixed-trough design. The fixed-trough Archimedes screw design has the screw rotate within a fixed concrete, or steel-lined trough with a small, intentional gap left between the blade tips and the trough. The gap is set at a width ( $G_w$ ) large enough that wearing and friction losses are minimized, yet small enough to also minimize losses associated with leakage flow through the gap (i.e., gap leakage,  $Q_g$ ). Figure 3 shows the layout of a modern screw pump station; the figure is annotated with the variables and parameters often used to describe the design and operation of a modern, conventional Archimedes screw.

Archimedes screws are often described by their geometric parameters, including the outer diameter ( $D_o$ ), inner diameter ( $D_i$ ), pitch ( $S$ ), length ( $L$ ), inclination angle ( $\beta$ ), gap width ( $G_w$ ) and number of blades ( $N$ ) (Figure 3). Screw pumps are also described by their operating parameters, like their rotation speed ( $\omega$ ), upper ( $h_U$ ) and lower ( $h_L$ ) water levels, and total deliverable flow rate ( $Q$ ).

Archimedes screw geometry plays a clear role in the structural mechanics of the system. The modern screw has a

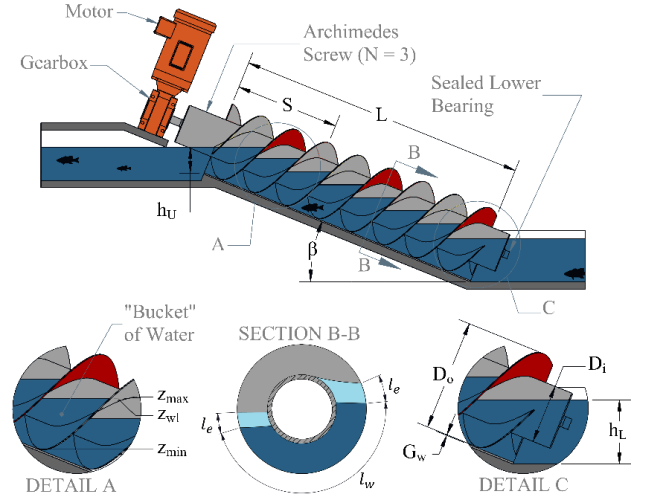


Figure 3. Archimedes screw pump dimensions and layout.

complex geometry: a hollow cylindrical tube capped with shaft hubs on each end, set at an incline, with blades welded helically along most of its length. Analytically, the state-of-the-art literature recommends neglecting the screw blades and performing structural calculations as if the screw were an inclined, simple span beam with a hollow, cylindrical cross-section [2]. It has been alleged that the blades add no helpful supporting characteristics to the screw structure, though no evidence was provided to support the claim [2].

It is hypothesized that the addition of screw blades might not reinforce the screw's structure, and that in increasing the screw's weight, it will increase deflection. So, additional screw blades may have an adverse structural impact on the screw and require a larger blade-trough gap to support increased deflection. The finite element analysis (FEA) performed in this study will investigate the impact of a varying number of blades for an otherwise identical screw geometry.

## II. EXPERIMENTAL METHODOLOGY

The tested screw was made of ASTM A500 Grade B/C steel. Its inner cylinder was constructed from round, hot rolled, hollow structural section tubing with a 4" outer diameter and .125" walls (equivalent to 101.6 mm and 3.175 mm, respectively). The tubing was cut to a length of 1460 mm and two .25" (6.35 mm) end caps were welded to seal the cylinder and affix hubs for a shaft to mount between bearings. Three blades were welded axially along the screw at equal radial spacing for a total flighted axial length of 48". Screw dimensions are reported in Table 1.

TABLE I. LABORATORY-SCALE ARCHIMEDES SCREW DIMENSIONS

$D_o$ (m)	$D_i$ (m)	$S$ (m)	$L$ (m)	$N$ (-)
0.316	0.102	0.317	1.219	3

The screw was mounted between two rolling element bearings that were press fit into wooden sawhorses made of dimensional lumber (Figure 4). The assembly was set on top of a rigid, solid oak work bench. Though the work bench and

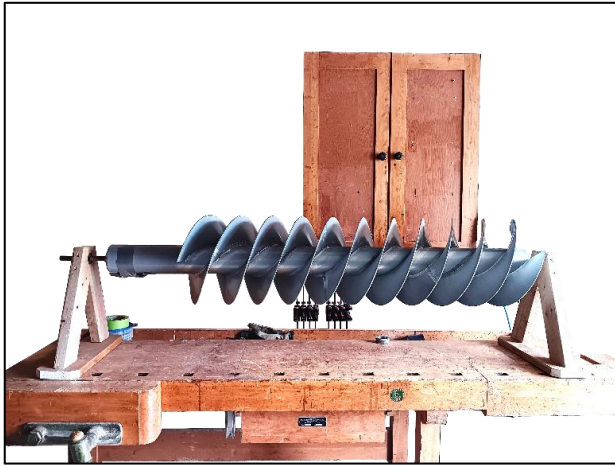


Figure 4. Experimental apparatus – a laboratory-scale Archimedes screw held on bearings between two sawhorses on an oak workbench.

sawhorses were rigid, they were still subject to some flexion due to the nature of their construction material. This introduced some unwanted experimental uncertainty, though it yielded the advantage of minimizing costs for this preliminary investigation.

Analogue indicators were affixed to the workbench and set against the screw at three locations along its length (corresponding to Figure 7). Three 0 to 1 inch dial indicators (Power Fist #2970986) were used to measure deflection in the screw (Figure 5). The indicators measured in increments of 1 thousandth of an inch (0.0254 mm). From the right-side fixture (see Figure 4), the indicators were placed at 6.35 cm, 69.4 cm, and 151.5 cm.

Two lengths of 1" polyester webbed strapping with vinyl-coated S-hooks were used to fasten a load to the centre of the Archimedes screw in the experimental fixture. Experiments began with a baseline, zero-load case. Next, a 20 litre, rigid high-density polyethylene bucket was fastened to the webbed strapping via the S-hook (see Figure 6). With the bucket empty, another set of measurements were taken to measure the bucket's no-load case.



Figure 5. Dial indicator mounted to apparatus and engaged on the Archimedes screw's inner cylinder.

After the zero-load conditions and baseline measurements were taken, the experiment was iterated while increasing loads. To increase the applied load on the screw, a volume of water was collected in a beaker and weighed. The water volume was then added to the 20-litre bucket and the beaker was once again weighed to determine the net weight of applied load that was added to the bucket. This number was recorded along with the dial indicators' measurements of deflection along the length of the screw. This process was iterated until the 20 litre bucket was full.

Altogether, it took 22 iterations to fill the bucket, so at least 22 datapoints were collected in total. Data was gathered for loads ranging from 0 N to 212 N, by increments of roughly 10 N.

It was mentioned that the use of a wooden workbench and sawhorses were very cost effect at the expense of introducing higher levels of experimental uncertainty. For this preliminary analysis, that was required to be a tolerable trade-off.

Experimental error was estimated to be 0.970 mm under maximum loading conditions during testing. The dial indicator had a measurement error of  $\pm 0.0127$  mm.

Measurement uncertainty associated with the wooden fixture was estimated by approximating the stiffness of the dimensional lumber sawhorses and the oak workbench. The oak workbench was built in Quebec and was likely constructed from white oak, which was estimated to have a modulus of elasticity of 12.3 GPa. This corresponded to an estimated maximum tested body displacement of 0.00246 mm.

The dimensional lumber was purchased in southern Ontario and designated as SPF lumber (spruce-pine-fir). This designation is often applied to white spruce, Engleman spruce, red spruce, black spruce, jack pine, lodgepole pine, balsam fir, and (sub)alpine fir. Conservatively, the least stiff wood species was selected to estimate the maximum potential displacement. The most elastic SPF wood species had a modulus of elasticity of 8.89 GPa. This corresponded to an estimated maximum tested body displacement of 0.955 mm.



Figure 6. A 20 litre bucket was filled with water to increase and decrease loading for the validation experiments.

### III. NUMERICAL METHODOLOGY

SolidWorks Simulation (SolidWorks Corp., 2023) was used in this study to perform static simulations on the Archimedes screw domain. SolidWorks Simulation had the benefits of being readily available to the researchers and having a familiar platform, all while having a high degree of reliability. All solvers included in SolidWorks Simulation have been benchmark tested and validated by the independent National Agency for Finite Element Methods and Standards (NAFEMS). Particularly for the static simulations used in this study, the solver will produce results with the same quality as other, more venerable finite element analysis software packages.

An Archimedes screw was modelled in SolidWorks (SolidWorks Corp., 2023). The model was given the same dimensions as the experimental screw (see Table 1). End caps, hubs, and the three screw blades were modelled as separate bodies so they could be assigned bonded contact with the inner cylinder, simulating the real-world welded connections.

The screw was meshed using SolidWorks Simulation's tetrahedral node elements. A higher level of refinement was applied near the screw end caps and other transition regions to improve accuracy in regions of interest. Figure 7 shows the three planes at the same locations corresponding to the dial indicators used in the experiments. To prevent the development of stress-singularities in the simulation, all sharp transitions were treated with at least a minimal radiused feature (i.e., a fillet or sharp edge break).

The simulation was set with fixtures to simulate bearings on each end of the screw. The lower end of the screw (right side of Figure 7) had boundary conditions that prevented radial and torsional motion. It also had a boundary condition on the shaft shoulder that prevented axial motion. The upper end of the screw (left side of Figure 7) was given boundary conditions on its shaft that prevented only radial motion, ensuring that boundary conditions were not over-defined.

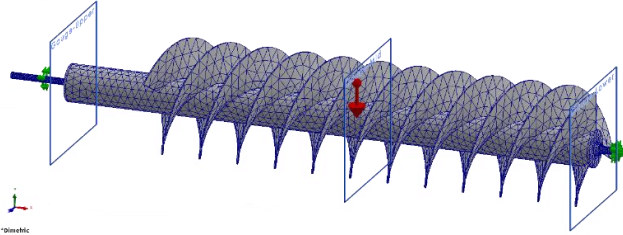


Figure 7. Simulation domain with mesh overlayed. The location of the three dial indicators used in the experiments are overlayed as 3 planes.

Split lines were used to create surface areas corresponding to the strapping used to fix the load on the screw experimentally (see Figure 6). A distributed load was applied on this surface area. Gravitational acceleration was supplied as a condition in the simulation; alongside material properties and inherent volume, this yielded weight characteristics and their impact on the simulation.

A mesh sensitivity analysis was performed to determine an appropriate mesh for the simulations. The maximum displacement was recorded (top-left, Figure 8) for the varying mesh sizes. However, considering the potential for stress-

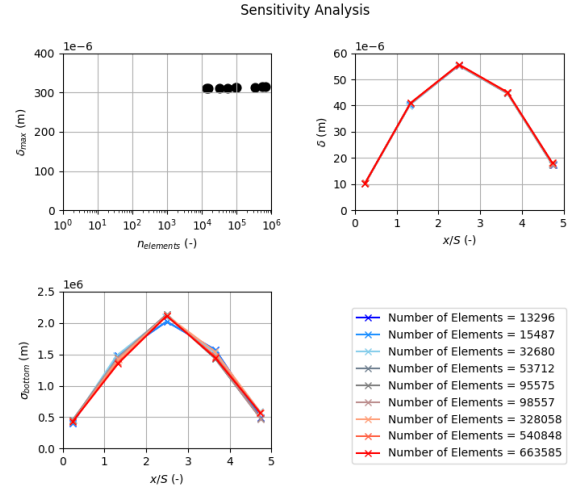


Figure 8. Sensitivity analysis results showing maximum deflection against number of elements (top left), deflection over the dimensionless length of the screw (top right), and von Mises stress over the dimensionless length of the screw (bottom left).

singularities to develop in the full domain, the region of interest was probed at five locations as well (top-right, Figure 8).

Considering deflection, it appeared that the results were always mesh-independent. The von Mises stress results were more impacted by mesh refinement levels (bottom-left, Figure 8). So, the authors used the stress results as an indicator of mesh sensitivity to yield a more reliable independent mesh refinement level. It was observed that the simulation became acceptably mesh-independent with 328058 elements, which seemed to be corroborated with the maximum displacement data as well.

### IV. RESULTS

The experimental results are presented in Figure 9 with dashed lines to help better visualize the data. Data is reported in dimensionless terms. The dimensionless distance along the screw is on the horizontal axis. It is the location of the dial indicator from the right-side fixture (see Figure 4) divided by the screw's pitch. In other words, it is the number of pitch lengths the dial indicator is away from the right-side fixture. The vertical axis presents the dimensionless deflection. Deflection was

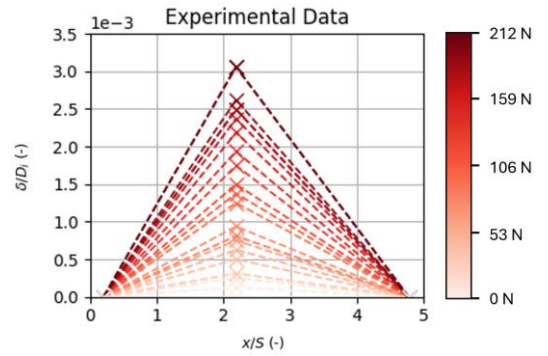


Figure 9. Experimental results presented as dimensionless deflection over the dimensionless length along the screw.



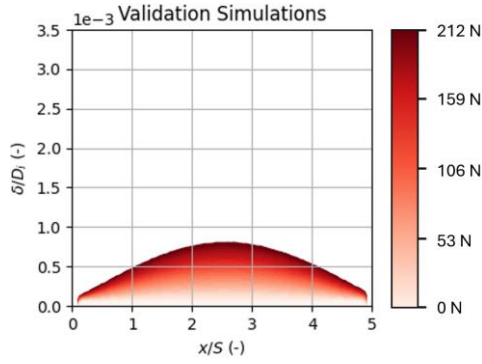


Figure 10. Simulation results presented as dimensionless deflection over the dimensionless length along the screw.

normalized by dividing by the inner diameter of the screw (Table 1). The term is thus analogous to strain.

It was observed that the deflection increased roughly linearly with the applied load, as should be expected. The highest recorded deflection was 0.432 mm while the screw was under 212 N of load.

Simulated data was normalized with the same methods. The non-dimensional simulation results are presented in Figure 10.

Simulated results showed similar trends to experimental observations. The deflection appeared to increase linearly with the applied load. The very reasonable and expected deflection response lent some credence to the accuracy of the simulation results.

The results had an average relative error of 0.786, which was not excellent. However, the dimensional difference between simulation and experiment was between 0.01 mm and 0.356 mm, which was well within experimental uncertainty. Based on the experimental uncertainty analysis proposed in the methodology, it seemed that deformation in the lumber apparatus had the potential to be much higher than the deformation of the screw under the tested loading conditions.

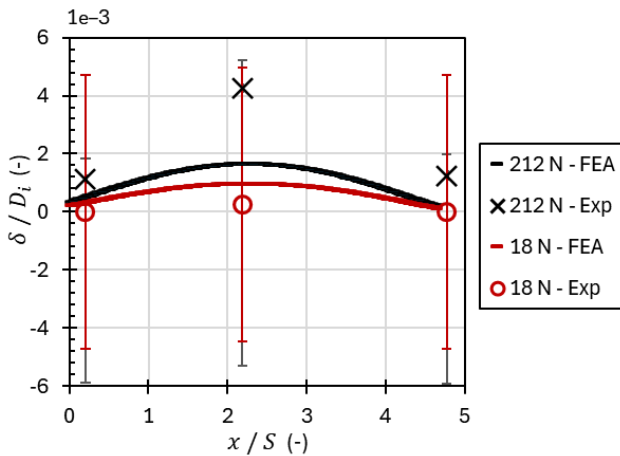


Figure 11. Comparison of experimental results and simulated results for the 18 N and 212 N runs. Results are presented as dimensionless deflection over the dimensionless length along the screw. Experimental data are presented with error bars to aide in model evaluation.

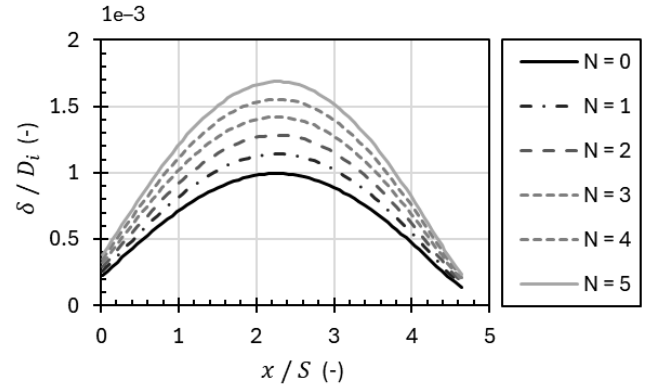


Figure 12. Impact of number of screw blades on deflection. Data is presented as dimensionless deflection over the dimensionless length along the screw for the six variations.

Direct comparisons with error bars were drawn between all simulation and experimental runs. It was easiest to visualize and compare higher-magnitude data, so the data corresponding to a load of 212 N is shown in Figure 11. The comparison was overlayed with the results for the 18 N data as well to demonstrate the high degree of experimental uncertainty and how it was impacted by loading.

It is considered that, though the simulations did not yield nominal results similar to the experimental results, there was a very high degree of experimental uncertainty. Though the results do not agree well, they do not discount the validity of the simulation. Since overall trends were in the correct direction, of the right form, fixturing was sensible, and it was a simple, static simulation, the authors suggest that the FEA model was a reasonable approximate projection of the structural response and deformation of an Archimedes screw under various loading schemes.

Using the new preliminary structural model, the authors explored the impact of number of blades on an Archimedes screw's structural response. Simulations were run at 212 N with  $N = 0, 1, 2, 3, 4$ , and 5 blades to observe the impact of blades on deflection (Figure 12). Finite element analysis was an excellent tool to use for this comparison since it was very costly to manufacture a range of unique screws for testing. Using numerical techniques provides valuable insight, especially for preliminary investigations, while incurring much lower costs.

It was observed that the addition of blades to the simulated Archimedes screw increased deflection. Since the loading characteristics did not change, it is suggested that this was due

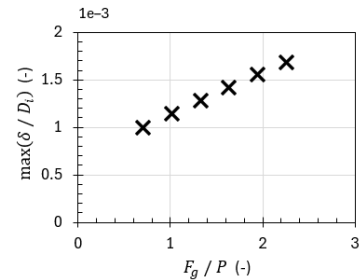


Figure 13. Impact of normalized screw weight on maximum dimensionless deflection.

to the addition of weight with each blade. Each blade of the screw weighed approximately 6.69 kg, with the experimental three-bladed screw weighing about 35.3 kg. To investigate this further, the weight of the screw ( $F_g$ ) was normalized by the applied load ( $P$ ) and compared against the maximum dimensionless deflection observed for the screws with varying number of blades (Figure 13).

A direct linear correlation was found between weight and maximum deflection in the FEA results. This suggests that the hypothesis of additional blades increasing deflection, rather than reinforcing the screw, may be true.

## V. CONCLUSION

This study was a very important first step in ongoing efforts to perform structural analyses in Archimedes screws. There currently exists no literature exploring the structural mechanics of Archimedes screws in any useful capacity for engineers and designers.

An example of the benefits of making improvements in this field include designing Archimedes screws with more precise blade-trough gaps. With more precise design, both leakage and frictional losses could be further minimized as well as yielding an increased lifespan of the screw trough and installation.

This study demonstrated a proof-of-concept for structural analysis of Archimedes screws. It will serve as the foundation for ongoing investigations to optimize the design of Archimedes screws for eco-friendly hydropower generators (Archimedes screw generators), and dewatering in a climate-impacted future (Archimedes screw pumps).

In this preliminary study, it was clear that screw geometry played a very important role in the structural mechanics of the system. Ongoing structural analysis will focus on varying screw geometric parameters including: system size (larger screws), diameter ratio, pitch ratio, length ratio, and inclination angle.

## ACKNOWLEDGMENTS

The authors gratefully acknowledge Tony Bouk and Brian Weber of Greenbug Energy Inc. (Delhi, Canada) for their continued help and support. This work was completed as one element of the larger research project "Improving Efficiency of Archimedes Screw Pumps" funded by the Natural Sciences and Engineering Research Council (NSERC) of Canada, Alliance program, grant ALLRP 561188-20.

## REFERENCES

- [1] D. Z. Haman, "Pumps, Displacement," in *Encyclopedia of Water Science*, B. A. Stewart and T. A. Howell, Eds., ed. New York: Marcel Dekker, 2003.
- [2] G. Nagel, *Archimedian Screw Pump Handbook: Fundamental Aspects of the Design and Operation of Water Pumping Installations using Archimedian Screw Pumps*. Schwäbisch Gmünd: RITZ-Pumpenfabrik OHG, 1968.
- [3] D. Siculus, "Bibliotheca Historica, Book I," in *Loeb Classical Library 279*, C. H. Oldfather, Ed., ed. Cambridge: Harvard University Press, c. 60 BCE/1933.
- [4] D. Siculus, "Bibliotheca Historica, Book V," in *Loeb Classical Library 340*, C. H. Oldfather, Ed., ed. Cambridge: Harvard University Press, c. 50 BCE/1939.
- [5] A. Naucratis, "Deipnosophistae, Book V," in *Loeb Classical Library 208*, C. B. Gulick, Ed., ed. Cambridge: Harvard University Press, c. 200/1928.
- [6] L. Euler, "De cochlea Archimedis," *Novi Commentarii academiae scientiarum Petropolitanae*, vol. 5, pp. 259-298, 1760.
- [7] Vitruvius, "De architectura, Book X," M. H. Morgan, Ed., ed. Cambridge: Harvard University Press, c. 25 BCE/1914.
- [8] S. Dalley and J. P. Oleson, "Sennacherib, Archimedes, and the water screw: The context of invention in the ancient world," *Technology and Culture*, vol. 44, no. 1, pp. 1-26, January, 2003 2003, doi: <https://www.jstor.org/stable/25148052>.
- [9] J. Muysken, "Berekening van het nuttig effect van de vijzel," *De Ingenieur*, vol. 21, pp. 77-91, 1932.
- [10] E. A. Asli-Ardeh and A. Mohsenimanesh, "Determination of effective factors on power requirement and conveying capacity of a screw conveyor under three paddy grain varieties," *The Scientific World Journal*, 2012, doi: DOI: 10.1100/2012/136218.
- [11] E. D. Weber, S. M. Borthwick, and L. A. Helfrich, "Plasma Cortisol Stress Response of Juvenile Chinook Salmon to Passage through Archimedes Lifts and a Hidrostral Pump," *North American Journal of Fisheries Management*, vol. 22, no. 2, 2002, doi: [https://doi.org/10.1577/1548-8675\(2002\)022<0563:PCSROJ>2.0.CO;2](https://doi.org/10.1577/1548-8675(2002)022<0563:PCSROJ>2.0.CO;2).
- [12] G. Nagel and K.-A. Radlik, *Wasserförderschnecken: Planung, Bau und Betrieb von Wasserhebeanlagen*. Berlin: Pfiemer Buchverlag in der Bauverlag, 1988.
- [13] M. J. Neumeyer and B. D. Jones, "The Marsh Screw Amphibian," *Journal of Terramechanics*, vol. 2, no. 4, pp. 83-88, 1965, doi: [https://doi.org/10.1016/0022-4898\(65\)90133-3](https://doi.org/10.1016/0022-4898(65)90133-3).
- [14] F. Crimson, "A. Archimedes Screw Vehicles," in *U.S. Military Tracked Vehicles*, G. H. Dammann Ed. Osceola: Motorbooks International, 1992, ch. Marginal Terrain Vehicles.
- [15] M. DiFrangia, "The hydraulics of injection molders," presented at the Fluid Power World, Cleveland, May 23, 2016, 2016.
- [16] L. B. Kreuziger and M. P. Massicotte, "Adult and pediatric mechanical circulation: a guide for the hematologist," *Hematology: The American Society of Hematology Education Program*, vol. 2018, no. 1, pp. 507-515, Nov 30, 2018 2018, doi: 10.1182/asheducation-2018.1.507.
- [17] S. C. Simmons, L. Miller, and W. D. Lubitz, "Review and Evaluation of Archimedes Screw Pump Design Guidance," in *Responsible Engineering and Living*, D. S. Ting and A. Vassel-Behagh Eds. Cham: Springer Proceedings in Energy, 2022.
- [18] J. W. P. Campbell, "The Development of Water Pipes: A Brief Introduction from Ancient Times until the Industrial Revolution," presented at the The Eighth Annual Conference of the Construction History Society, Queens' College, Cambridge, 2021.